Volume 12 Number 24 1984 Nucleic Acids Research

DNA structural variations produced by actinomycin and distamycin as revealed by DNAase I footprinting

Keith R.Fox and Michael J.Waring

Department of Pharmacology, University of Cambridge, Medical School, Hills Road, Cambridge CB2 2QD, UK

Received 26 October 1984; Accepted 23 November 1984

ABSTRACT

The technique of DNAase I footprinting has been used to investigate preferred binding sites for actinomycin D and distamycin on a 160-base-pair DNA fragment from E.coli containing the tyr T promoter sequence. Only sites containing the dinucleotide step GpC are protected by binding of actinomycin, and all such sites are protected. Distamycin recognizes four major regions rich in A+T residues. Both antibiotics induce enhanced rates of cleavage at certain regions flanking their binding sites. These effects are not restricted to any particular base sequence since they are produced in runs of A and T by actinomycin and in GC-rich sequences by distamycin. The observed increases in susceptibility to nuclease attack are attributed to DNA structural variations induced in the vicinity of the ligand binding site, most probably involving changes in the width of the helical minor groove.

INTRODUCTION

A family of techniques, collectively known as "footprinting", have been used to investigate the sequence-selectivity of DNA binding ligands such as actinomycin, echinomycin, chromomycin and distamycin [1-7]. Sites to which the antibiotic is bound are protected from cleavage by a chemical reagent or DNAase I and are visualized at single bond resolution as gaps in the autoradiograph of a denaturing polyacrylamide gel, revealing both the position and length of each ligand binding site. The method requires that the footprinting agent be capable of cleaving all internucleotide bonds, so that inhibition at every site can be detected. DNAase I, however, does not cleave all DNA sequences at identical rates: it tends to produce a sequence-dependent pattern of cleavage in duplex DNA without any preference for a particular base [8]. Nevertheless, although the use of DNAase I yields footprinting patterns which are harder to interpret, the enzyme can be employed to investigate local variations in DNA structure as well as the precise location of preferred antibiotic binding site(s) [8,9].

It has recently been reported that the bifunctional intercalating

antibiotic echinomycin can induce conformational changes in sequences flanking some of its binding sites, resulting in enhanced susceptibility to cleavage by DNAase I [4]. This effect has been interpreted in terms of the antibiotic altering the width of the narrow groove at nearby sequences, thus affecting the rate of cleavage by DNAase I at such sites. Weaker enhancement effects have also been reported for triostin A and its des-N-tetramethyl derivative TANDEM [10], structurally similar compounds. A careful examination of previous work with actinomycin also reveals facilitated cleavage at a few sites although this has not been discussed in detail [1,3].

There is a wealth of information concerning gross structural changes induced in DNA by ligand binding [11] as well as several crystallographic studies which portray the precise structures of drug-oligonucleotide complexes [12-14]. However, much less is known about the extent of conformational changes produced by ligand binding: whether they are restricted to the actual binding site, or whether they can be distributed over neighbouring regions of DNA. In this paper we examine the DNAase I footprinting patterns produced by two well-known, but widely differing ligands: actinomycin D and distamycin A. Actinomycin has been reported to bind to the dinucleotide sequence GpC [15-17] and in previous footprinting studies was also found to inhibit cleavage at CpC and GpG [3]. Distamycin binds to AT-rich regions [1,6,18]. These footprints provide information about the exact location of the antibiotic binding sites as well as structural alterations induced in flanking sequences.

MATERIALS AND METHODS

Antibiotics and enzymes

Distamycin hydrochloride was a gift from Dr. F. Arcamone, Farmitalia, Italy. Actinomycin D was a product of Merck Sharp and Dohme. Antibiotic solutions were freshly prepared by direct weighing and dissolved in 10 mm tris-HCl, pH 7.5, containing 10 mM NaCl. Deoxyribonuclease I (DNAase I) was obtained from Sigma and prepared as a 7200 units/ml stock solution in 0.15M NaCl containing 1 mM $MgCl_2$. It was stored at -20°C and diluted to working concentrations immediately before use. The digestion buffer used to dilute the enzyme contained 20 mM NaCl, 2 mM $MgCl_2$ and 2 mM $MnCl_2$. Mn^{2+} was used together with Mg^{2+} because it speeds up the cutting rate 50-fold without causing any change in the control DNA digestion pattern [9].

3'-End labelling with reverse transcriptase

The 160 base-pair duplex DNA fragment from E.coli containing the tyrosine tRNA promoter together with its adjacent sequences was isolated and labelled as previously described [4]. Incubation with reverse transcriptase, dGTP and α-[^{32}P] dCTP led to selective radioactive labelling of the 3' end of the "Watson" (sense) strand (upper sequence in Figure 2). Incubation with reverse transcriptase, dTTP and α-[^{32}P] dATP led to selective labelling of the 3'-end of the "Crick" strand (lower sequence in Figure 2).

Synthesis and 5'-end labelling of a 20-mer

The 20-mer shown in Figure 5 (a gift from Dr. H.R. Drew) was synthesised by the solid-state phosphotriester method, and purified by electrophoresis on 20% (w/v) denaturing polyacrylamide gels. Product bands were cut out, soaked in 0.3M sodium acetate and precipitated twice with ethanol. The oligomers were 5'-end labelled as previously described [9] using bacteriophage T4 polynucleotide kinase. Excess buffer and salt were removed from the final product by ethanol precipitation. The structure of the strands was confirmed by standard sequencing methods [9].

DNAase I footprinting

Samples (3 µl) of the labelled tyr T fragment (9 pmoles in base pairs) were incubated with 5 µl of antibiotic solution (5-40 µM) at 37°C for 30 mins then digested with 2 µl of DNAase I (final concentration 0.01 units/ml). 3 µl Aliquots were removed from the mixture after 1, 5 and 30 mins digestion and the reaction stopped by adding 2.5 µl of 80% formamide containing 0.1% bromophenol blue and 10 mM EDTA. Samples were heated at 100°C for at least 2 min prior to electrophoresis. An identical procedure was used for footprinting the labelled 20-mer in the presence of distamycin except that the final antibiotic concentration was only 5 µM and the incubation was performed at room temperature.

Gel electrophoresis

The products of tyr T digestion were analysed on 0.3 mm 8%(w/v) polyacrylamide gels containing 7M urea and tris-borate EDTA buffer, pH 8.3. After 2 hours electrophoresis at 1500V the gel was soaked in 10% acetic acid for 10 mins, transferred to Whatman 3MM paper, dried under vacuum at 70°C and subjected to autoradiography at -70°C with an intensifying screen. The 20-mer digests were analysed on 20% (w/v) polyacrylamide gels containing 7M urea. After 3h electrophoresis the gel was covered with Saran wrap and subjected to autoradiography. Bands in the tyr T digestion

pattern were assigned by comparing the pattern in control lanes with that previously determined [4,8,10].

Densitometry

Autoradiographs were scanned using a Joyce-Loebl microdensitometer to produce profiles from which the relative intensity of each band was measured. For the tyr T fragment data are expressed as fractional cleavage (f) = A_i/A_t as previously described [4, 10], where A_i is the area under band i and A_t is the sum of the intensity under all bands in any gel lane. When comparing different digestion patterns in this way, care was taken to ensure that the extent of digestion was similar and limited to 20-40% of the starting material so as to minimize the incidence of multiple cuts in any strand. Data from this analysis are presented in the form of ln ($f_{antibiotic}$) - ln ($f_{control}$), representing the differential cleavage at each bond relative to that in the control. The results are displayed on a logarithmic scale for convenience so that positive values indicate enhancement, negative values blockage. The autoradiographs from the 20-mer were analysed in terms of probabilities of cleavage by the method of Lutter [19], correcting for any multiple cutting that might have occurred (see legend to Figure 5). Again the analysis was limited to digestion patterns in which the fraction of starting material remaining was as high as possible.

RESULTS

Actinomycin D

Typical DNAase I digestion patterns for the 160-mer tyr-T duplex in the presence and absence of actinomycin (AMD) are displayed in Figures 1a and 1b for the upper (Watson) and lower (Crick) strands respectively. Each gel lane contains about 100 bands which can reasonably be resolved; these were analysed as described in the methods section, giving rise to the differential cleavage plot shown in Figure 2. It is immediately apparent that the cleavage pattern in the presence of the antibiotic is very different from that of the DNA alone, and five sites protected by the antibiotic can easily be discerned. It is also evident that the rate of cleavage at certain bonds is strongly enhanced relative to that in the control.

The five sites protected by the antibiotic are located near positions 132, 119, 100, 75 and 36 and can be clearly seen on both strands. At each site the block is staggered across the two strands by about three bonds

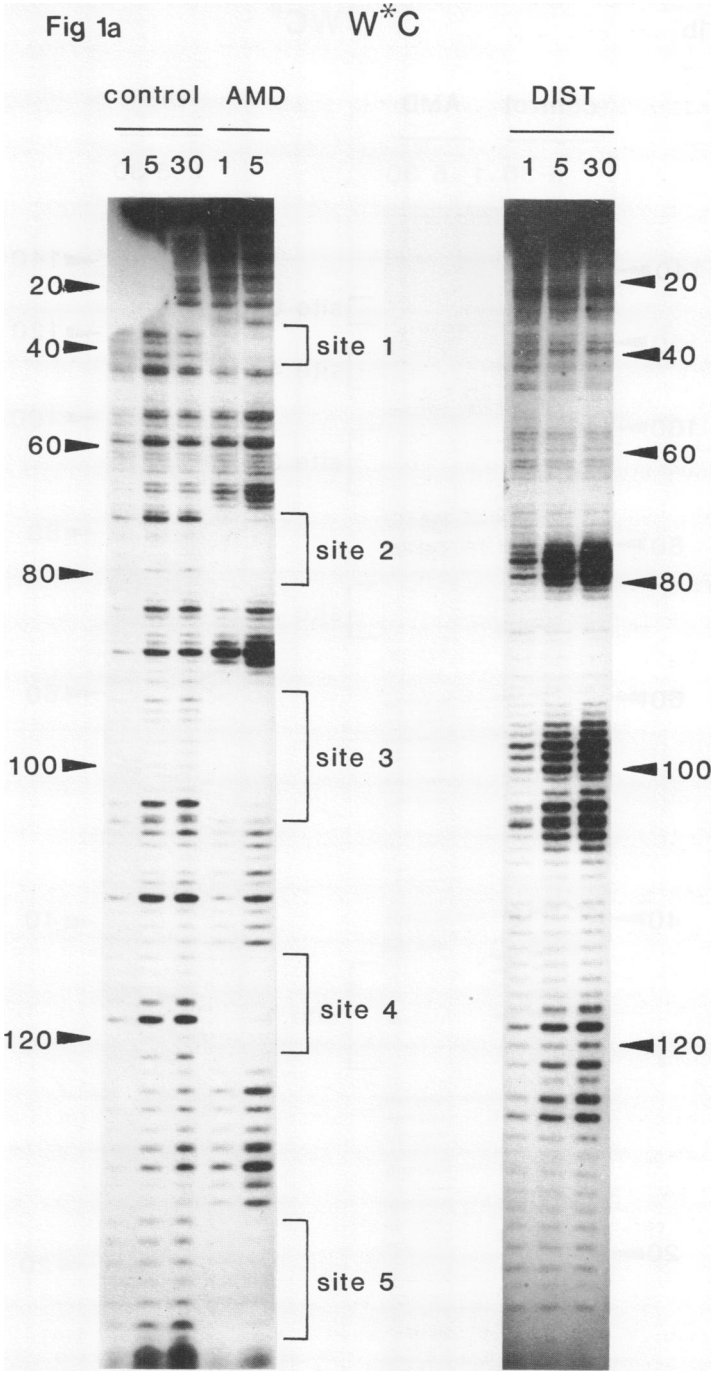
Fig 1a
W*C
control
AMD
DIST
1 5 30 1 5
1 5 30
20
40
60
80
100
120
site 1
site 2
site 3
site 4
site 5

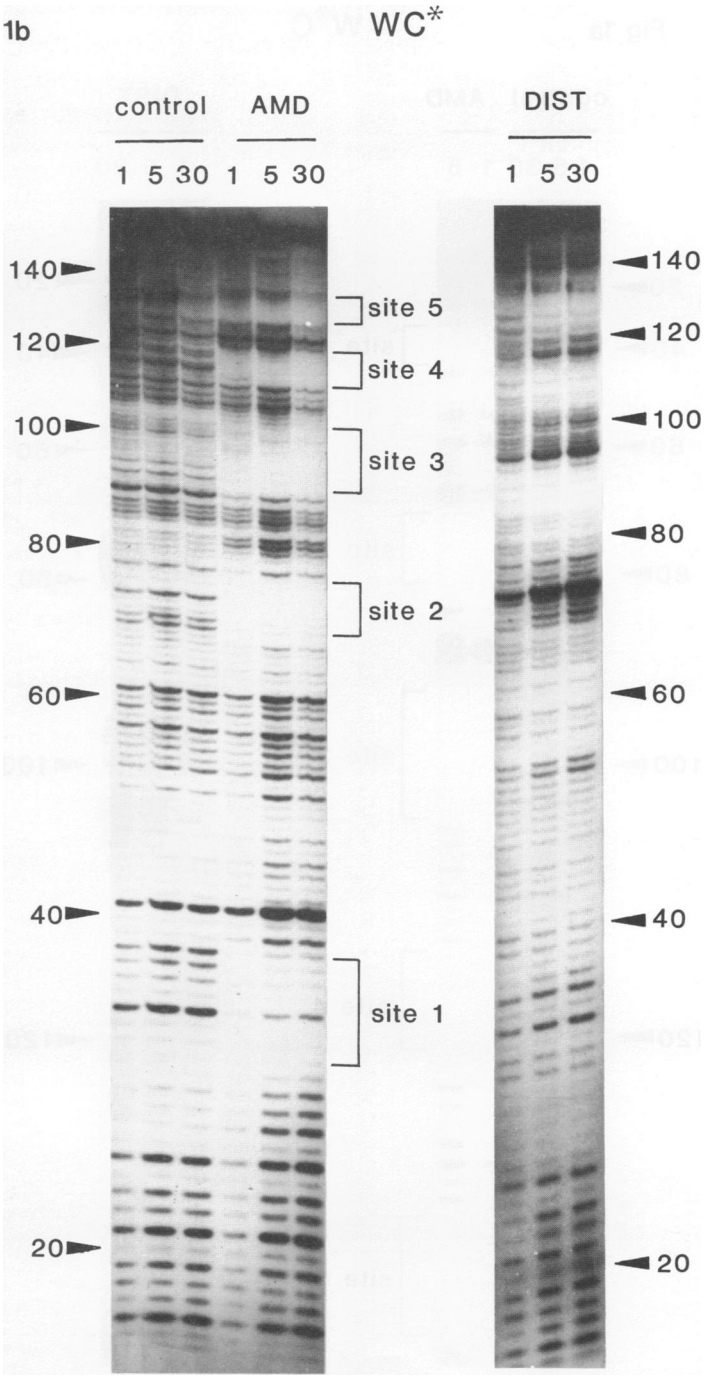
1b
WC*
control
AMD
DIST
1 5 30 1 5 30
1 5 30
140
120
100
80
60
40
20
site 5
site 4
site 3
site 2
site 1
140
120
100
80
60
40
20

towards the 3' end, as previously observed with DNAase I footprinting [4], presumably because DNAase I cuts bonds which lie in close proximity across the double-helical minor groove. As anticipated each site contains the dinucleotide sequence GpC, and all such sequences are protected. By way of contrast, the dinucleotide sequences CpC and GpG are often left unprotected; examples being at positions 23, 40, 106 and 113. It is not possible to assess the exact size of the region protected by each bound ligand since three of the sites contain more than one dinucleotide step of the type GpC. However, the inhibition of cleavage around positions 36 (site 1) and 132 (site 5) extends over about 6-8 base-pairs. Experiments performed with different concentrations of actinomycin revealed that below 3 μM no significant protection was evident and that between 5-20 μM the pattern remained constant. At sites 2 and 4 which both contain multiple binding sites the GpC steps are not affected to the same degree. For example, the GpC step at position 117 is better protected than the neighbouring step at position 121, suggesting that the antibiotic binds preferentially to one site only, thereby excluding binding at the other.

The regions where cleavage by the enzyme is enhanced in the presence of the antibiotic are rich in A+T residues, and lie in positions where the enzyme does not cut the native DNA very well. They are similar, but not identical, to the regions where cutting is enhanced in the presence of echinomycin [4]. In every case the enhanced cutting occurs adjacent to sites where actinomycin is bound, suggesting that the effect results from some distortion of the local DNA structure to a form more susceptible to cleavage, generated by the binding of the ligand. However, not every bound ligand provokes the same effect since, for example, no change in cutting rate is apparent between sites 3 and 4. The broad region of enhancement between sites 1 and 2 extends over about 25 base pairs, perhaps with a break around position 57, suggesting that the ligand-induced effect can be propagated in either direction from the binding site over more than one turn of the DNA helix.

Figure 1. DNAase I footprinting of actinomycin D (AMD) and distamycin (DIST) on the 160-base-pair DNA fragment whose sequence is represented in Figure 2. Symbols W*C in Figure 1(a) and WC* in Figure 1(b) indicate which of the two strands (Watson or Crick) bears a radioactive 3'-end label. Time in minutes (1, 5, 30) after the addition of the enzyme is shown at the top of each gel lane. Numbers refer to the numbering scheme of Drew and Travers [8] used in Figures 2 and 3. The conditions of digestion were as described in the methods section using an antibiotic concentration of 5 μM in each case.

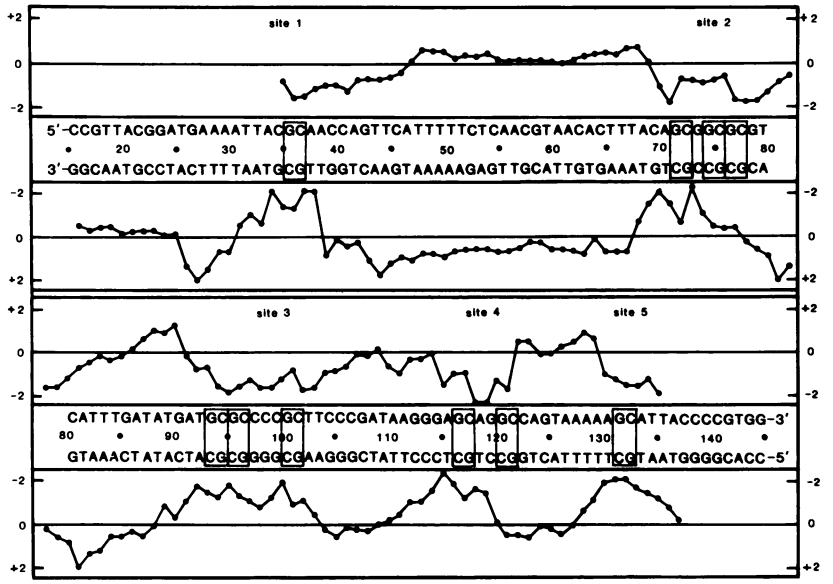

Figure 2. Differential cleavage plot for actinomycin-induced differences in susceptibility to DNAase I digestion. The upper Watson strand reads 5' to 3' left-to-right, while the lower Crick strand reads 5' to 3' right-to-left. Vertical scales are in units of $\ln(f_a) - \ln(f_c)$, where f_a is the fractional cleavage at any bond in the presence of antibiotic and f_c is the fractional cleavage of the same bond in the control, for closely similar extents of overall digestion. Positive values indicate enhancement, negative values blockage.

Since both echinomycin and actinomycin enhance the cleavage at similar regions of the DNA the question arises as to whether these putative long range perturbations are restricted to AT-rich sequences or whether other ligands which bind to AT-rich regions can alter the cutting rate at flanking GC-rich sites. In order to investigate this question we chose to examine DNAase I footprinting patterns in the presence of an AT-selective ligand.

Distamycin

DNAase I digestion patterns measured in the presence of distamycin are displayed in Figures 1a and 1b alongside those for actinomycin, and the intensity of resolved bonds is represented in the form of a differential cleavage plot in Figure 3. With distamycin at least four protected sites are readily visible, each centred around an AT-rich region. However, it is not easy to assess accurately the extent of blockage produced by the

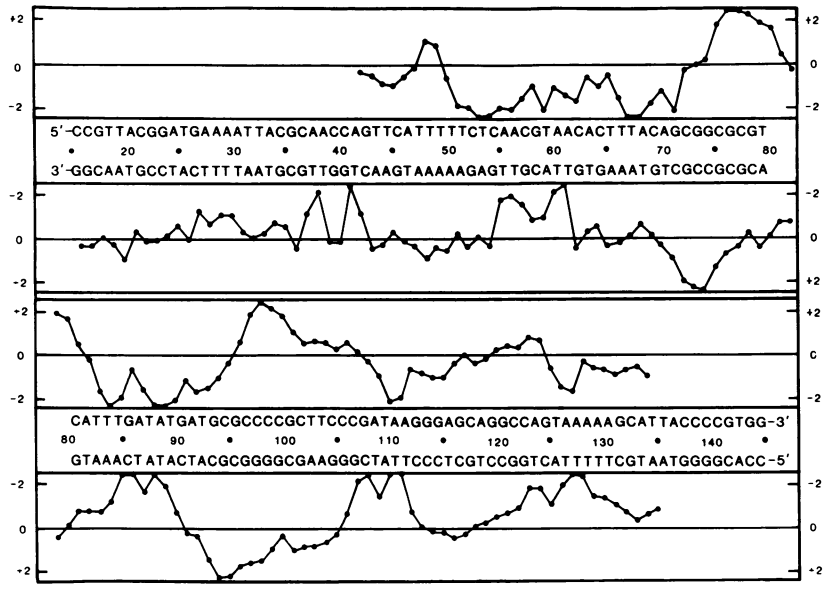

Figure 3. Distamycin-induced differences in susceptibility to DNAase I digestion. Symbols are as described in the legend to Figure 2.

antibiotic since these protected zones occur at sites where DNAase I cuts the native DNA with low efficiency. This is especially noticeable around positions 35 and 50, regions designated as "gap 1" and "gap 2" by Drew and Travers [8].

More impressive than these blockages are the very pronounced enhancements of cleavage around positions 75 and 97. Both occur in GC-rich regions of the DNA and again lie in areas where DNAase I cuts the native DNA at a lower than average rate. It therefore appears that distamycin too can induce changes in regions of DNA flanking some of its binding sites. The possible structural origin of these differences will be considered in the discussion.

As with actinomycin, not every bound distamycin molecule produces an enhancement of cutting at flanking sequences. For example no enhancement can be seen on the Crick strand from positions 0-70 although this region contains one if not two strong distamycin binding sites.

Footprinting of a 20-mer

In order to investigate further the effect of distamycin binding on the structure of adjacent GC-rich regions we have examined DNAase I

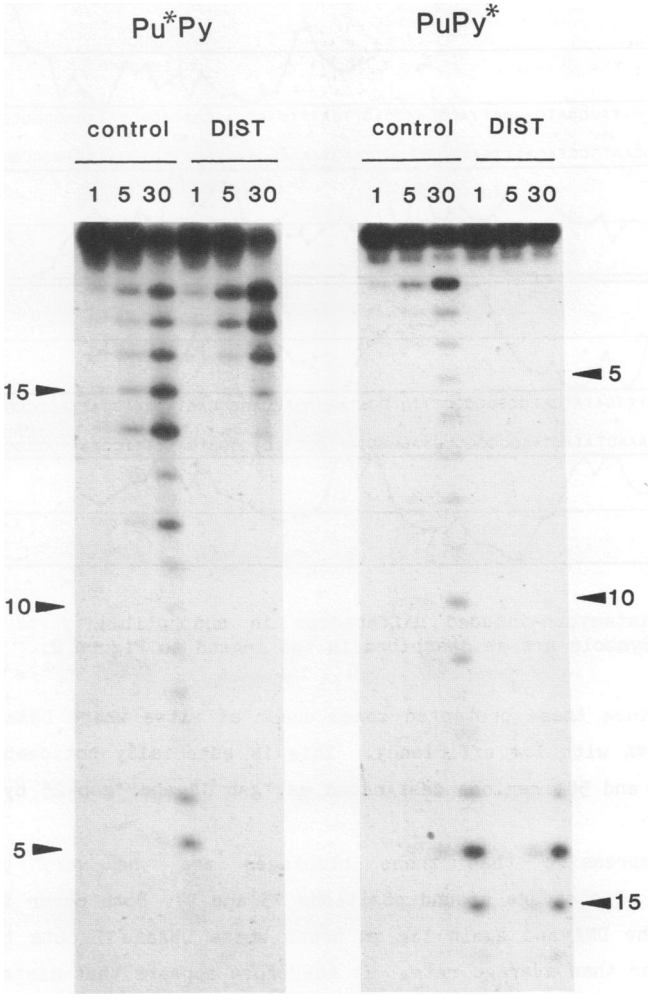

Figure 4. DNAase I digestion patterns of the 20-mer (for sequence and numbering scheme see Figure 5) in the presence and absence of 5 μM distamycin. Symbols Pu*Py and PuPy* indicate which of the two strands (purine or pyrimidine) contains the 5'-end label. Time in minutes after the addition of enzyme is shown at the top of each gel lane.

digestion patterns derived from a synthetic DNA 20-mer of sequence $GA_{11}G_8$ in the presence and absence of the antibiotic. With this DNA, designed specifically to probe the effect of neighbouring DNA sequences on each other, cutting at the G's is visibly efficient (Figures 4 and 5) by virtue of their proximity to the long run of A's [H.R. Drew, personal

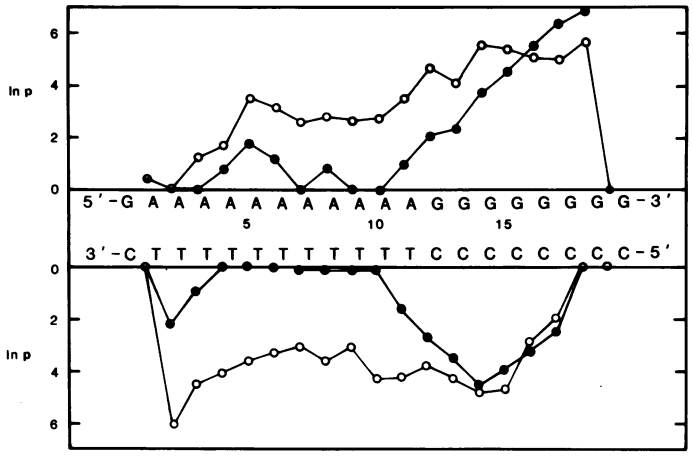

Figure 5. Relative probability of cleavage of 20-mer in the presence (•) and absence (o) of distamycin, expressed on a logarithmic scale. Probabilities were calculated by the method of Lutter [19] using single-time-point data derived from microdensitometer tracings of the autoradiographs in Figure 4. In this procedure, the areas R_i under bands in any gel lane are first summed to give the total area (or radioactivity) R_t, then converted to fractions of total cleavage $f_i = R_i/R_t$. True probabilities of cleavage are determined from these fractional distributions by correcting for the incidence of cuts between bond i and the radioactively labelled end, as described by Drew and Travers [8].

communication]. We were therefore interested to discover whether cutting at these regions could be further enhanced by binding of distamycin to the neighbouring AT-rich sequence.

The observed digestion patterns are displayed in Figure 4 and the calculated relative probabilities of cleavage are presented in Figure 5. Cleavage of this synthetic oligonucleotide by DNAase I proceeds more rapidly in the run of G.C pairs than in the corresponding A.T region. By comparison, in the tyr-T DNA fragment runs of A and runs of G are both poorly cleaved by DNAase I, thought to be because the minor groove is too narrow in the former and too wide in the latter to bind the enzyme efficiently [8]. However, the GC region of our synthetic oligomer is cut reasonably well, presumably because the flanking AT segment has altered its conformation, forcing it to adopt a structure more like mixed sequence DNA. The effect of distamycin on the 20-mer cleavage pattern is to reduce markedly the cutting at the AT region. The GC-rich section, which is already cut well, shows little enhancement apart from a slight increase at the 3' end of the purine strand. This lack of any major enhancement

demonstrates that such effects are not a necessary consequence of distamycin binding but depend on the precise environment of sequences surrounding the binding site.

DISCUSSION

Sequence preferences

The present results have helped to clarify those base sequences which form the preferred binding sites for actinomycin and distamycin. Actinomycin, at concentrations between 3 and 20 μM, protects the DNA from enzymic cleavage only around the sequence GpC. Other studies have suggested that actinomycin footprints may also be centred around GpG and CpC [3]. However, protection of GpG and CpC was only detected at higher antibiotic concentrations and may reflect secondary, less tight, binding. In contrast distamycin protects from DNAase I cleavage at regions which are rich in A+T residues. This is in accord with previous results using MPE-Fe(II) as a footprinting agent [1,6]. However, the regions of enhanced cleavage are only apparent using DNAase I.

A more accurate assessment of the binding of these ligands is not possible from the present results for several reasons. Firstly, distamycin binds best to regions of DNA which are poorly cut by DNAase I so that further blockages are hard to detect. Secondly, actinomycin-binding sites on this particular DNA fragment occur mainly in clusters. Thirdly, DNAase I is perhaps not the best probe for estimating the limiting site size for DNA-binding ligands [2]. However, the sensitivity of DNAase I to the precise local structure of the DNA can be turned to advantage insofar as it is capable of yielding information not easily available using a less selective footprinting agent such as MPE-Fe(II).

Structural changes upon binding

Our results suggest that a common property of sequence-selective DNA-binding ligands lies in their ability to induce structural changes in regions surrounding some of their binding sites, leading to an enhanced rate of cleavage by DNAase I. These effects are not restricted to any particular base sequence since distamycin enhances the rate of cleavage at certain GC-rich regions while actinomycin and echinomycin enhance the cleavage at runs of A and T. In each instance the increased cutting occurs at regions where DNAase I cuts with low efficiency presumably because such regions normally exist in a rather resistant conformation which returns to a more "normal" structure under the influence of the neighbouring bound ligand. Clearly this type of enhancement can not be possible at all

sequences since if the DNA is already cut well by DNAase I and is in the optimal conformation for recognition by the enzyme any structural perturbations can only result in a decreased rate of cleavage.

What then is the structural basis for these enhanced rates of cleavage? It has been suggested [8,9] that DNAase I binds across the minor groove of the double helix and that local variations in groove width might affect the cutting efficiency of the enzyme. By comparing the observed cutting efficiency with X ray crystal structures of short DNA fragments Drew and Travers [8] surmised that the native enzyme cuts poorly at runs of A and T because these nucleotides are associated with a narrow minor groove on account of the high propeller twist of the steps AA, AT and TT. By contrast, the efficiency of cutting at GC regions may be low because the minor groove is wider than average. A simple model to explain the antibiotic-induced enhancement of nuclease attack is that, when this occurs in an AT-rich region, it is because the neighbouring ligand has induced a local widening of the minor groove, possibly because the base pairs have been flattened out. Enhancement at GC runs would result from reducing the local groove width.

Is this model consistent with the known effects of ligands on the winding of the DNA helix? A recent study with netropsin, which is structurally related to distamycin, led to the conclusion that it produces a small local winding of the DNA [20], an effect which if transmitted to neighbouring sequences is likely to reduce the width of the minor groove. Moreover, a crystal structure of netropsin bound to a DNA dodecamer [14] has revealed that it binds to the sequence AATT, and that the width of the minor groove at this point is 10Å, markedly low compared with the normal value of 12-13Å taken from the B-DNA fibre model [21]. On the other hand intercalators such as actinomycin and echinomycin are known to unwind DNA [22,23]. If part of the total unwinding is distributed over neighbouring sequences, as well as those directly involved at the binding site, then there would be an effective local widening of the narrow groove. It is worth noting that the unwinding angle of DNA-binding ligands determined by changes in superhelical density of covalently closed circular DNA will include contributions from both the local and longer range structural alterations whereas crystal structures of short oligonucleotide-drug complexes will only evidence the local effect.

It should be emphasised that the enhancement effects demonstrated here are much more pronounced (and extensive) than any previously reported for other DNA-binding ligands [1, 3, 4, 10]. This is partly attributable to the

nature of the DNA fragment employed here, which happens to contain a substantial number of runs of A/T and G/C sequences which appear to adopt peculiar helical structures, and also because DNAase I is a more sensitive probe of local DNA structure than other footprinting tools such as MPE-Fe(II). However, enhancements can also be detected using this simpler reagent as is evident from a careful examination of the published MPE-Fe(II) footprinting patterns of echinomycin [5]. Once again, enhanced cleavage can be detected at certain AT-rich regions, consistent with our interpretation that the structural alterations are real and not just a consequence of using DNAase I.

Theory of Footprinting

The sites protected from cleavage by actinomycin and other large DNA-binding drugs are probably the result of ligand molecules physically blocking the access of the enzyme to the DNA-phosphate backbone. However, the protection afforded by distamycin may not be so simply explained. The crystal structure of a netropsin-DNA dodecamer complex shows that the ligand lies well within the minor groove where it effectively replaces a "spine" of water molecules [14], so that access of DNAase I to the phosphate backbone might not be restricted. In this case it is possible that protection from enzyme cleavage might arise because the minor groove is trapped in a relatively narrow conformation by the binding of the ligand, such that it can no longer accommodate the enzyme. Indeed, it is possible to mimic the distamycin-induced pattern of nuclease cleavage merely by exposing the native oligomer to DNAase I at low temperature (H.R. Drew, personal communication).

It is interesting to speculate why the enhancement of enzymic cleavage produced by various similar DNA binding ligands varies so much in intensity. We note that the dissociation rate constants increase in the order actinomycin, echinomycin, triostin A, TANDEM [24-27], the inverse ranking order of the strength of the enhancement effects. It is possible that persistence time and nuclease enhancement may be correlated in the sense that ligands which persist for longer on the DNA, thereby causing long-lived perturbation(s) of the helical structure, produce the strongest enhancement of cleavage.

ACKNOWLEDGMENTS

We thank Dr Horace Drew and Mrs Loretta Low for their help and encouragement. The work was supported by grants from the Cancer Research Campaign, The Royal Society and the Medical Research Council.

REFERENCES

[1] Lane, M.J., Dabrowiak, J.C. and Vournakis, J.N. (1983) Proc. Natl. Acad. Sci. USA 80, 3260-3264.
[2] Van Dyke, M.W. and Dervan, P.B. (1983) Nucleic Acids Res. 11, 5555-5567.
[3] Scamrov, A.V. and Beabealashvilli, R.Sh. (1983) FEBS Letters 164, 97-101.
[4] Low, C.M.L., Drew, H.R. and Waring, M.J. (1984) Nucleic Acids Res. 12, 4865-4879.
[5] Van Dyke, M.W. and Dervan, P.B. (1984) Science 225, 1122-1127.
[6] Van Dyke, M.W., Hertzberg, R.P. and Dervan, P.B. (1982) Proc.Natl. Acad. Sci. USA 79, 5470-5474.
[7] Van Dyke, M.W. and Dervan, P.B. (1983) Biochemistry 22, 2373-2377.
[8] Drew, H.R. and Travers, A.A. (1984) Cell, 37, 491-502.
[9] Drew, H.R. (1984) J. Mol. Biol. 176, 535-557.
[10] Low, C.M.L., Olsen, R.K. and Waring, M.J. (1984) FEBS Letters, in press.
[11] Waring, M.J. (1981) Annu. Rev. Biochem. 50, 159-192.
[12] Neidle, S. (1981) in Topics in Nucleic Acid Structure, Part I, Neidle, S. ed., pp. 177-196, Macmillan, London.
[13] Wang, A.H-J., Ughetto, G., Quigley, G.J., Hakoshima, T., van der Marel, G.A., van Boom, J.H. and Rich, A. (1984) Science, 225, 1115-1121.
[14] Kopka, M.L., Yoon, C., Goodsell, D., Pjura, P., and Dickerson, R.E. (1984) manuscript submitted for publication.
[15] Sobell, H.M. and Jain, S.C. (1972) J. Mol. Biol. 68, 21-34.
[16] Sobell H.M. (1973) Progr. Nucl. Acid Res. Mol. Biol. 13, 153-190.
[17] Krugh, T.R., Mooberry, E.S. and Chiao, Y-C.C. (1977) Biochemistry 16, 740-755.
[18] Zimmer, C. (1975) Progr. Nucl. Acid Res. Mol. Biol. 15, 285-318.
[19] Lutter, L.C. (1978) J. Mol. Biol. 124, 391-420.
[20] Snounou, G. and Malcolm, A.D.B. (1983) J. Mol. Biol. 167, 211-216.
[21] Arnott, S. and Hukins, D.W.L., (1972) Biochem. Biophys. Res. Commun. 47, 1504-1510.
[22] Waring, M.J. (1970) J. Mol. Biol. 54, 247-279.
[23] Waring, M.J. and Wakelin, L.P.G. (1974) Nature 252, 653-657.
[24] Krugh, T.R., Hook, J.W., Lin, S. and Chen, F-M. (1979) in Stereodynamics of Molecular Systems (Sarma, R.E., ed.), pp. 423-434, Pergamon Press, New York.
[25] Fox, K.R., Wakelin, L.P.G. and Waring, M.J. (1981) Biochemistry 20, 5768-5779.
[26] Fox, K.R., and Waring, M.J. (1981) Biochim. Biophys. Acta 654, 279-286.
[27] Fox, K.R., Olsen, R.K. and Waring, M.J. (1982) Biochim. Biophys. Acta, 696, 315-322.